

Jan Wiesenthal

IÖW

Energy-Prosumer-Model

Overview of the model, methodology and data basis

Working Paper, Version 1.0

Berlin, August 2023



Imprint

Publishers:

Institute for Ecological Economy Research (IÖW)

Institut für ökologische Wirtschaftsforschung GmbH, gemeinnützig

Potsdamer Straße 105

10785 Berlin

Germany

Phone: +49 – 30 – 884 594-0

Fax: +49 – 30 – 882 54 39

E-Mail: mailbox@ioew.de

www.ioew.de

Acknowledgement

The Energy-Prosumer-Model was developed by a number of people. I like to thank in particular: Mark Bost, Swantje Gähns, Jonas von Braunmühl, Paula Cremerius, Anselm Eicke, André Presser, Daniel Rimkus, Evelin Wieckowski and Andreas Wolfmaier.

The publication was funded by the German Federal Ministry of Education and Research within “SteuerBoard Energie” (Grant No. 01UU2005B)

Supported by:



on the basis of a decision
by the German Bundestag

Abstract

The Energy-Prosumer-Model is used to simulate energy flows within a household or a neighborhood. The model is a bottom-up simulation model with the possibility to select different generation, storage and/or consumption modules in a household or a neighborhood. The simulation can be applied in a number of different locations and years. The Energy-Prosumer-Model is particularly well suited for exploring technology options and operating scenarios with regard to self-consumption, self-sufficiency, power feed-in, and power purchase of electricity at the local level. The model was developed in 2010 and has been continuously enhanced and extended with new functionalities for a variety of different use cases. This documentation reflects the current state of development and will be updated regularly. Hence, this documentation can be understood as a living document. On the heating side, the underlying functions, assumptions, inputs and outputs of heating circuit, thermal storage, electric heater, condensing boiler, heat pump and solar thermal are described. On the electric side the modules photovoltaic, wind turbine and battery are described.

The Author

Jan Wiesenthal

Researcher

Institute for Ecological Economy Research

Contact: Jan.Wiesenthal@ioew.de

Tel. +49 – 30 – 884 594-38

Contents

1	Introduction	7
1.1	Functionality and brief description	7
1.2	Simulation environment.....	8
1.3	Classification in the model landscape, application area and limitations	9
1.4	Target user group.....	9
2	Environmental parameters	13
2.1	Environmental data imported in the model	13
2.2	Radiation on an inclined surface.....	13
2.2.1	Input.....	14
2.2.2	Angle of incidence	14
2.2.3	Radiation on an inclined surface	15
2.2.4	Reflected radiation on an inclined surface.....	16
3	Simulation of energy demand of households and communities	17
3.1	Heating demand.....	17
3.2	Hot water demand.....	18
3.3	Electricity demand.....	19
4	Simulation of heat production and storage	22
4.1	Control.....	22
4.2	Heating circuit	23
4.2.1	Input.....	23
4.2.2	Flow temperature.....	24
4.2.3	Power calculation.....	25
4.3	Thermal storage	25
4.3.1	Input.....	26
4.3.2	Flow allocation	26
4.3.3	Convection	26
4.3.4	Storage temperature.....	27
4.4	Electric heater	28
4.5	Condensing boiler	29
4.5.1	Input.....	29
4.5.2	Utilization rate	29
4.5.3	Power calculation.....	30
4.6	Heat pump.....	30
4.6.1	Input.....	31
4.6.2	Flow temperature.....	31
4.6.3	Power calculation.....	31
4.7	Solar thermal.....	32
4.7.1	Input.....	32
4.7.2	Flow temperature.....	32
4.7.3	Power calculation.....	33

5	Simulation of electricity production and storage	34
5.1	Photovoltaic	34
5.1.1	Input.....	34
5.1.2	Cell temperature	34
5.1.3	Electric power	35
5.1.4	Inverter	36
5.2	Wind.....	36
5.2.1	Input.....	36
5.2.2	Wind speed at hub height.....	37
5.2.3	Electric power	38
5.3	Battery.....	39
5.3.1	Input.....	39
5.3.2	Charging and discharging of the battery	39
6	Output and post-processing.....	40
7	References	41

List of Figures

Fig. 1.1: Resolution flowchart of EProM.....	8
Fig. 1.2: EProM load profile	10
Fig. 1.3: EProM used to simulate use of battery storage.....	11
Fig. 1.4: Self-sufficiency in energy sharing communities depending on demand side management and origin of electricity.....	12
Fig. 2.1: Radiation on an inclined surface flowchart	14
Fig. 3.1: Use of electricity in individual areas of households depending on number of people in household	20
Fig. 3.2: Standard load profile	21
Fig. 3.3: Yearly consumption	21
Fig. 4.1: Modeled heating components in EProM.....	22
Fig. 4.2: Heating circuit flowchart.....	23
Fig. 4.3: Thermal storage flowchart	26
Fig. 4.4: Condensing boiler flowchart.....	29
Fig. 4.5: Utilization rate of condensing boiler	30
Fig. 4.6: Heat pump flowchart	31
Fig. 4.7: Solar thermal flowchart	32
Fig. 5.1: Photovoltaic electricity production flowchart	34
Fig. 5.2: Wind turbine flowchart	36

List of Tables

Tab. 2.1: Environmental parameters used in EProM.....	13
Tab. 3.1: Floor area in single family houses per person in Germany	17
Tab. 5.1: Roughness of different types of landscapes.....	38

1 Introduction

The Energy-Prosumer-Model (EProM) is used to simulate energy flows within a household or a neighborhood. The model was developed at IÖW in 2010 and has been continuously enhanced and extended with new functionalities so that it can be used for a variety of different use cases. This documentation reflects the current state of development and will be updated regularly. Hence, this documentation can be understood as a living document. The goal of this documentation is to ensure that the underlying data are findable, accessible, interoperable and reusable in the spirit of good science in accordance with the FAIR principles (Wilkinson et al. 2016). As the model itself is not open source, it is all the more important that the sources and the functionality are transparent.

Accordingly, this documentation has three main goals:

1. Overview of the model's functionality
2. Overview of the used data and sources
3. Overview of the results to be achieved

1.1 Functionality and brief description

The model simulates energy flows within a household or a neighborhood on a minute-by-minute basis. The model is modular. Thus, it is possible to select different generation, storage and/or consumption modules for a household/neighborhood to be simulated. The electricity generation technologies include a photovoltaic (PV) system and a wind turbine. For heat generation, an electric heater, a solar thermal system, a heat pump, and a condensing boiler are used. For the storage of electricity or heat, a battery or a hot water tank is modeled. The consumption is composed of the consumption of electrical appliances and the demand for heat for space heating and hot water. The user can specify the use case by defining, for example, the year to be simulated, the size of the household or the capacity of a generation plant. The model then accesses stored data, such as weather data, information on the efficiency of generation plants, or load profiles of individual devices. Fig. 1.1 shows the resolution flowchart of EProM. Energy flows - electricity and heat - are visualized. A selection of input and output parameters are shown.

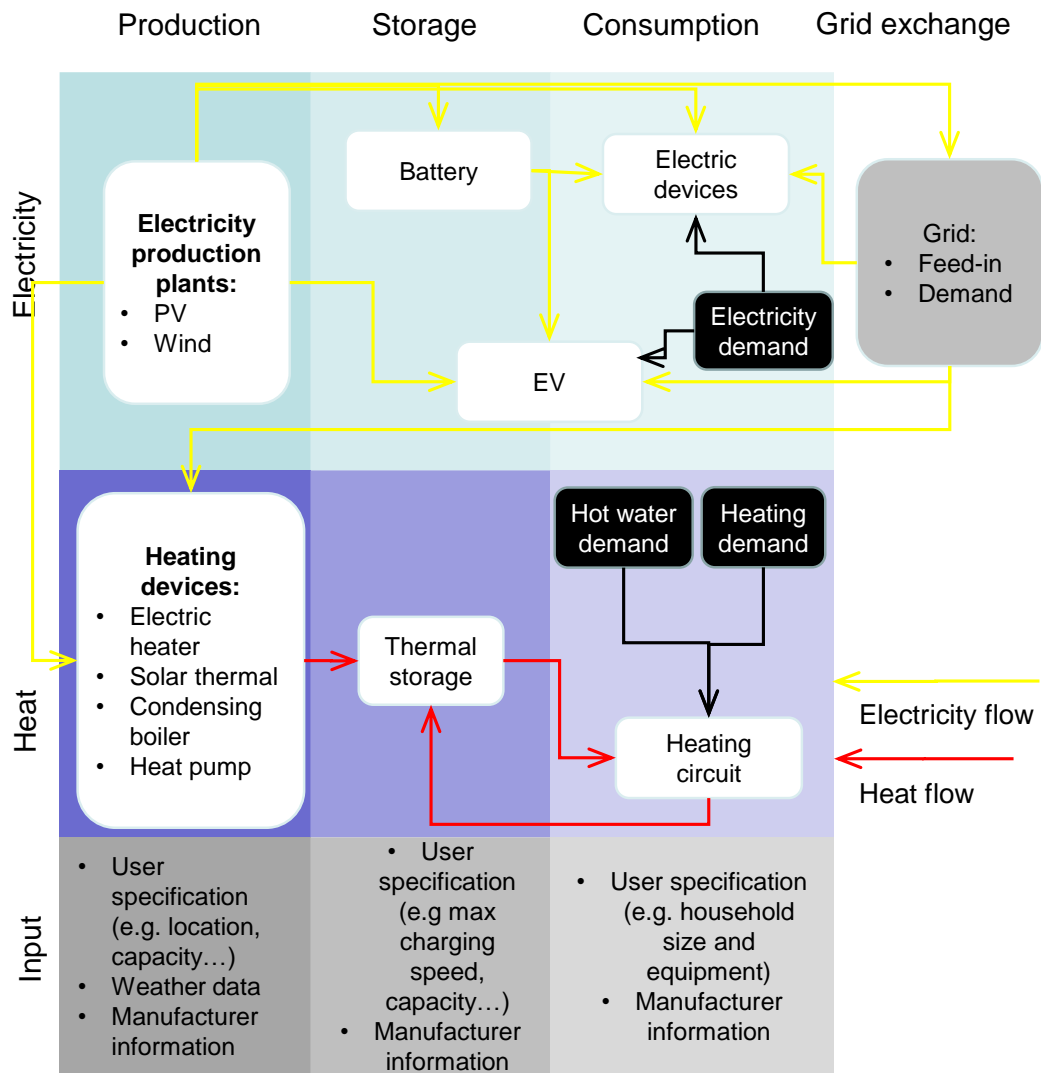


Fig. 1.1: Resolution flowchart of EProM

A detailed description of the underlying assumptions, parameters and user's input is given in the following chapters.

1.2 Simulation environment

The software used for the realization of the model is Simulink, a simulation tool from Mathworks. The scripts and underlying functions are written in Matlab R2022a. The fixed step size is 60 respectively to input and output on a minutely basis. The solver used is a fourth-order Runge-Kutta-method. The underlying solver is necessary especially for the calculation of the heating circuit, where a differential equation is solved in each time step (see Chapter 4.2.). In most of the other modules no differential equation has to be solved.

1.3 Classification in the model landscape, application area and limitations

Energy system models can be categorized in several ways. One of the most common distinctions is between top-down and bottom-up models (Grubb et al. 1993; Herbst et al. 2012; Nakata 2004). In this context, EProM can be classified as a bottom-up model. This is due to the very high level of detail of the technologies within the EProM model. Hence, the EProM model is not used to answer macroeconomic questions, as in the case of top-down models, but to perform economic and ecological assessments for specific simulated technologies. However, an element of a top-down approach is implemented when it comes to the electricity demand of an individual household. Although each electric device is modeled with an individual load profile, the sum of the total electricity demand in a household follows statistical distributions (see Chapter 3.3 electricity demand). In a way, this also represents a limitation of the model. When simulating multiple households, the individual load profiles are synthetically generated based on distribution. However, if the simulated households are in a neighborhood, simultaneity effects may occur.

Bottom-up models can be divided into the subcategories of optimization, simulation, multi-agent, and partial equilibrium models (Herbst et al. 2012). EProM belongs to the category of simulations. Thus, EProM is especially suitable for simulating specific use cases and is able to map the effects of individual decisions in an imperfect market as transparently as possible (Dieckhoff 2017). Due to the small time-step of one minute, EProM also reflects temporary peaks (e.g., simultaneous use of an electric kettle and an electric stove or temporary shading of the PV system by clouds). This can limit over- and underestimations that may occur with larger time step sizes using aggregated data. However, a minute-by-minute simulation also requires input data of high quality, which is not always available. For this reason, input data is only stored in the model for certain locations and years. In addition, very precise assumptions are made regarding usage frequencies and probabilities for individual devices. There is limited data available for these needed assumptions. Hence, these assumptions are based on different sources from different years.

1.4 Target user group

By including both the demand and production of a household or neighborhood, EProM is particularly well suited for exploring technology options and operating scenarios with regard to self-consumption, self-sufficiency, power feed-in, and power purchase of electricity at the local level. There, temporary effects of clouds and simultaneous use of devices play a more important role than calculations at the macro level, where aggregated data can also be used.

In the project “Analysis of Economic, Technical and Environmental Benefits of Energy Storage Systems in Grid-connected Photovoltaic Systems” conducted by ISEA, IFHT and IÖW the model was used for example to calculate the self-sufficiency and load shifting potential of PV systems in households.

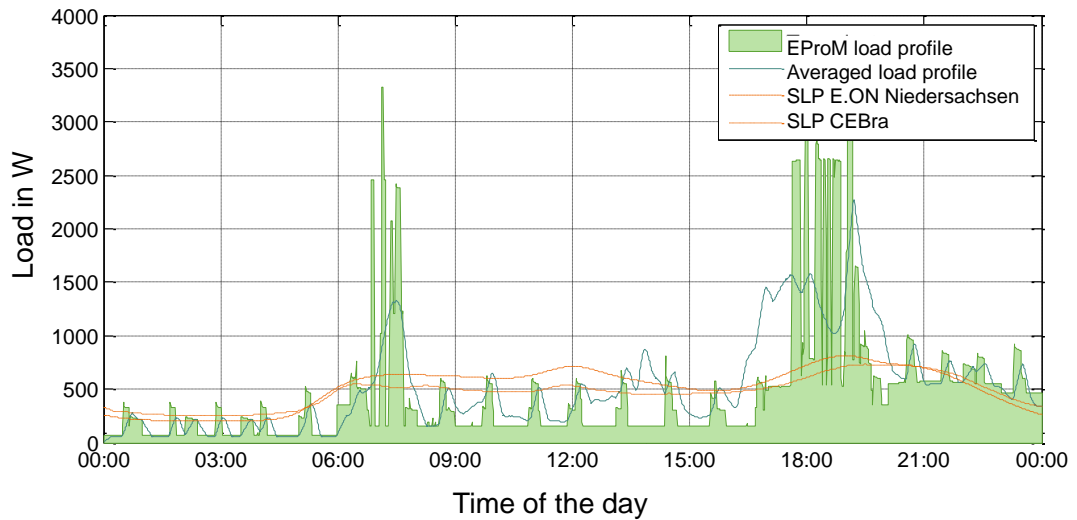


Fig. 1.2: EProM load profile

Source: Moshövel et al. (2015)

Moreover, EProM can be used to calculate changes in electricity demand and supply due to new technologies or possible changes in behavior. For example, in “Energy storage services for smart neighbourhoods (ESQUIRE)”, EProM was used to compare the use of home storage systems with community energy storage (see Fig. 1.3). This also allows new business models to be identified and evaluated.

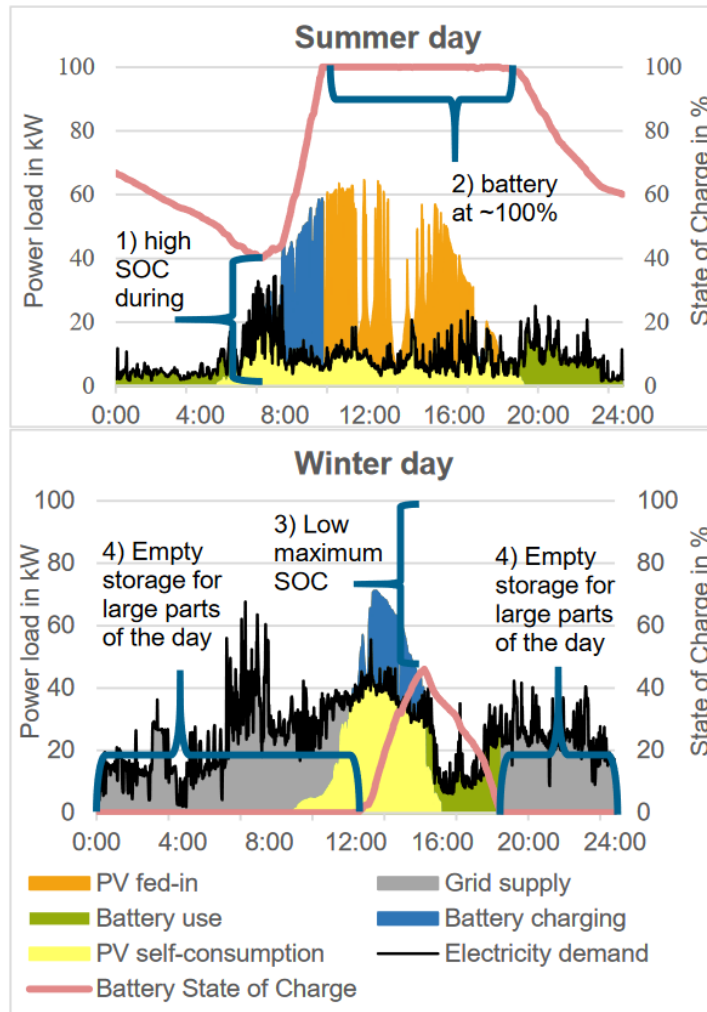


Fig. 1.3: EProM used to simulate use of battery storage

Source: Wiesenthal et al. (2022)

The results of the simulation can also feed into the ecological assessment - in particular the greenhouse gas emissions - and thus into policy recommendations for the promotion of one or the other technology in the sense of an optimization of a cross-technology subsidy policy.

In addition, the effects of policies on different electricity price components, such as grid charges, levies, etc., and the associated distribution effects can be measured when calculating self-consumption shares. For example, in the project “Energy Sharing a potential analysis”, EProM was used to simulate the share of electricity that energy communities can consume by generating electricity from different sources of electricity production units (see Fig. 1.4).

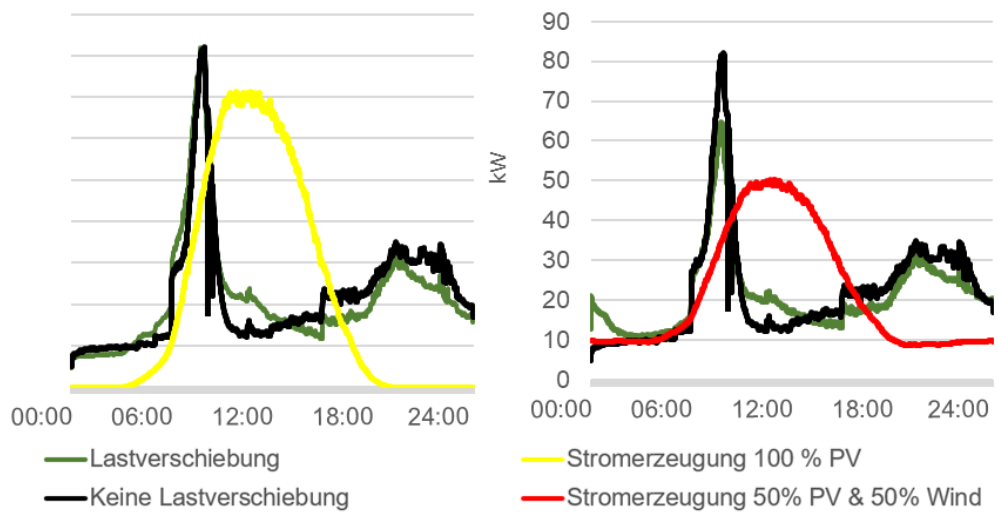


Fig. 1.4: Self-sufficiency in energy sharing communities depending on demand side management and origin of electricity

Source: Wiesenthal et al. (2022)

2 Environmental parameters

2.1 Environmental data imported in the model

Both demand and production calculations require environmental data. Tab. 2.1 gives an overview of the imported data with measurement location, year, time resolution and source.

Tab. 2.1: Environmental parameters used in EProM

Environmental parameter	Measurement location	Year	Time resolution	Sources
Diffuse radiation on the horizontal surface in W/m ² ,	Cabauw (CAB), Carpentras (CAR), Cener (CNR), Ford Peck (FPE), Lindenberg (LIN), Palaiseau (PAL),	2004: LIN	1 minute	Augustine (2017), Haeffelin (2017), Knap (2018), Olano (2017), Wacker and Behrens (2022)
Direct radiation on the horizontal surface in W/m ²		2013-2017: CAB, CAR, CNR, FPE, LIN, PAL, PAY		
Air temperature at 2 m height		2018: CAB		
Groundwater temperature	Germany	Ø2007-2010	monthly	Miara et al. (2012)
Wind speed	Lindenberg, Kiel, Stuttgart	2015	10 minutes	DWD (2019)
Air density	Lindenberg, Kiel, Stuttgart	2015	10 minutes	DWD (2019)

2.2 Radiation on an inclined surface

For different modules the radiation on an inclined surface is required. The direct, diffuse and reflected radiation imported into the model (see Tab. 2.1) must be transformed according to the inclination of the surface. Fig. 2.1 shows a simplified flowchart of the necessary calculations. A detailed description of the inputs and calculations follows.

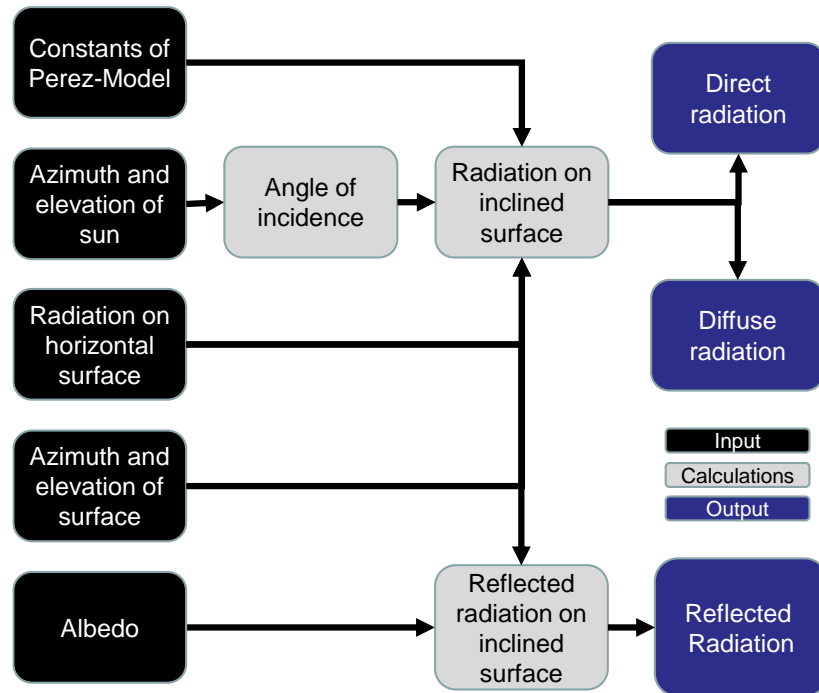


Fig. 2.1: Radiation on an inclined surface flowchart

2.2.1 Input

The simulation of the radiation on an inclined surface uses different inputs:

- **Azimuth and elevation of sun:** Calculated based on DIN 5034 using the longitude and latitude of the location and the time of the simulation
- **Azimuth and elevation of surface:** User input of the area illuminated by the sun
- **Radiation on a horizontal surface:** Depending on the selected location and modelled year (see Chapter 2.1)
- **Constants of Perez-Model:** From Quaschnig (2013) based on Perez-Model (Perez and Stewart 1986; Perez et al. 1987; Perez et al. 1990)
- **Albedo constant:** Parameter defining the fraction of sunlight reflected by a body (Quaschnig 2013)

2.2.2 Angle of incidence

To calculate the radiation on the surface, the angle of incidence has to be calculated. Eq. 2.1 from Quaschnig (2013) is used to calculate the angle of incidence.

Eq. 2.1: Angle of incidence of the sun according to Quaschnig (2013)

$$q_{incl} = \arccos(-\cos(\gamma_S) * \sin(\gamma_E) * \cos(\alpha_S - \alpha_E) + \sin(\gamma_S) * \cos(\gamma_E))$$

γ_S elevation of sun

γ_E elevation of surface

α_S azimuth of sun

α_E azimuth of surface

2.2.3 Radiation on an inclined surface

Eq. 2.2 is used to calculate the direct radiation on an inclined surface. Using the calculated angle of incidence, the direct radiation on a horizontal surface, and the elevation of the sun as input, the radiation on an inclined surface can be calculated.

Eq. 2.2: Direct radiation on an inclined surface according to Quaschnig (2013)

$$E_{dir,incl} = E_{dir,hor} * \frac{\cos(q_{incl})}{\sin(\gamma_S)}$$

$E_{dir,hor}$ direct radiation on a horizontal surface

q_{incl} angle of incidence

γ_S elevation of sun

To calculate the diffuse radiation on an inclined surface, Eq. 2.3 is used, as described by Quaschnig (2013) based on Perez et al (1986; 1987; 1990). For a detailed explanation of the Horizon Brightness Index and the Circumsolar Index, see Quaschnig (2013).

Eq. 2.3: Diffuse radiation on the inclined surface according to Quaschnig (2013)

$$E_{diff,incl} = E_{diff,hor} * \left\{ \frac{1}{2} * (1 + \cos(\gamma_E)) * (1 - F1) + \frac{a}{b} * F1 + F2 * \sin(\gamma_E) \right\}$$

$E_{diff,hor}$ diffuse radiation on a horizontal surface

γ_E elevation of surface

$F1$ circumsolar Index

$F2$ Horizon Brightness Index

A $\max(\cos q_{incl}; 0)$

B $\max(\sin \gamma_E; 0.087)$

q_{incl} angle of incidence

2.2.4 Reflected radiation on an inclined surface

To calculate the reflected radiation, a simplified approach proposed by Quaschnig (2013) is used. Using albedo coefficients, the global radiation on a horizontal surface, and the elevation of the surface, the reflected radiation is calculated. (see Eq. 2.4)

Eq. 2.4: Reflected radiation on an inclined surface according to Quaschnig (2013)

$$E_{refl,inl} = E_{G,hor} * A * \frac{1}{2} * (1 - \cos(\gamma_E))$$

$E_{G,hor}$ global radiation on a horizontal surface

A albedo coefficient

γ_E elevation of surface

3 Simulation of energy demand of households and communities

3.1 Heating demand

Total heating demand

The annual heating demand depends on the annual heating demand per m², the m² per person and the number of people in the household. Eq. 3.1 shows the calculation for the annual heating demand.

Eq. 3.1: Annual heating demand

$$E = \vartheta_B * m_{pp}^2 * P_{hh}$$

ϑ_B Annual heating demand per m² in kWh/m² per year

m_{pp}^2 Floor area per person

P_{hh} Number of people in household

Either the user provides input for heating demand per m² and floor area per person or average values are used in the model. Average heating demand per m² is based on total energy demand (Capros et al. 2016) and the share of energy for heating (Eurostat 2017). Average floor area per person is based on the German Federal Statistical Office (Statistisches Bundesamt 2019), which provides concrete values for average floor area for different household sizes (see Tab. 3.1). The relative differences in m² per person between household sizes are also used for other European countries to calculate the average floor area per person (see Rovers 2019).

Tab. 3.1: Floor area in single family houses per person in Germany

Data based on Statistisches Bundesamt (2019)

Number of people in household	m ² per household	m ² per person in household
1	104,7	104,7
2	128,1	64,05
3	137,4	45,8
4	147,4	36,85
5	158,4	31,68

Heating profile

For the simulation, a heating profile is generated on an hourly basis. Due to the inertia of the heating system, a higher resolution of the heating profile is not necessary. The generated daily profile is based on BDEW (2022) and combines:

1. A sigmoid profile based on Hellwig (2003) and
2. A linear part, which is visible in measured real load profiles.

Eq. 3.2 shows the calculation for the heating profile. In contrast to the BDEW (2022) calculations, the average daily temperature is not used. Instead, a weighted average of the temperature of the day and the previous day is used to account for the storage capacity of the building. Also, the hot water profile is calculated separately and is not included in this equation. Empirical parameters for households can be found in BDEW (2022). The user can choose between HEF33, HEF34, HMF33 and HMF34 profiles.

Eq. 3.2: Daily heat profile based on BDEW (2022)

$$h(\vartheta) = \frac{A}{1 + \left(\frac{B}{\vartheta_w - \vartheta_0}\right)^C} + m_H * \vartheta_w + b_H$$

A, B, C, D empirical Parameters

ϑ_w weighted average of temperature of the day and previous day

ϑ_0 reference temperature 40 °C

m_H empirical parameter reflecting slope of linear regression

b_H empirical parameter reflecting calibration point of linear regression

The hourly distribution of the daily heating demand is based on values provided by Hellwig (2003) for households. At the beginning of the simulation, the calculated heating profile is multiplied by the total heat demand.

3.2 Hot water demand

To calculate the hot water demand for the model, standard profiles are created according to Jordan and Vajen (2003) to distribute the demand over the day. DHWcalc has been developed for this purpose. It was developed as part of the International Energy Agency's "Solar Heating and Cooling Program" at the Technical University of Denmark and the University of Kassel. The model considers four different withdrawal reasons (short withdrawal, medium withdrawal, bath, shower). These are considered with different proportions of total consumption, frequencies per day, quantities per withdrawal, and quantities per minute. There are also different withdrawal probabilities. This depends on whether it is a weekend or a weekday. The simulation is based on the default values from the tool.

Deviating from this, the consumption for the average withdrawal quantities per day was calculated as follows:

- The input is an average consumption per day. This is determined based on the hot water demand in kWh (Eurostat 2017).
- The amount of hot water consumed per day (ϑ_N) can be calculated using Eq. 3.3.
- The groundwater temperature is assumed to be approximately equal to the mean air temperature (NGWA 1999). The years 2013 to 2017 were used to calculate the mean ground water temperature.
- The heated water is assumed to be 40 °C.

Eq. 3.3: Hot water consumption per day (VDI 2017)

$$\vartheta_N = \frac{q_N}{\rho * c(\vartheta_N - \vartheta_k)}$$

- q_N Energy demand per person per year (excluding distribution and storage losses)
- ρ Density of heated water
- c Heat capacity of water
- ϑ_N Temperature of heated water (40°C)
- ϑ_k Temperature of groundwater

3.3 Electricity demand

The electricity demand of the household is a combination of electricity used directly in the household and electricity used for heating. In this section, only the electricity demand for direct household use is described. In Chapter 4, the electricity demand for heating devices is explained.

The electricity demand of household devices is modeled bottom-up. A total of 29 devices with individual minute load profiles according to Reinhardt et al. (2012) are included in the model. For some devices, different randomly selected operating modes result in different load profiles, e.g. the washing machine has different load profiles depending on the program selection. The selection of simulated household devices in the specific application depends on the size of the household and the location of the household (Instituto Nacional de Estadística 2008; van Thiel 2017; Statistisches Bundesamt 2019; IDAE 2011).

The start times and duration of appliance use are simulated for each day individually. For most devices, the start time is randomized within a time interval distributed based on a normal distribution with a fixed variance. Hereby, the user's definition of the regular presence and absence of household members influences the time interval during which certain appliances might run. The user defines both vacation days and regular times during the day when the household members are present. For lighting, not only presence but also the outdoor brightness is relevant and is therefore calculated for each time step. In comparison, some loads of devices are independent of presence or absence. For example, the refrigerator and the freezer have the same variable load profile regardless of the presence or absence of household members.

The probability of devices being used depends on the day of the week (e.g., the stove is more likely to be used for lunch on the weekend than on a weekday), the season (e.g., dryer is less likely to be used in the summer) and the number of people in the household.

The sum of all modeled bottom-up profiles was adjusted according to three principles:

The frequency and duration of use of the individual appliances is chosen to match the average energy consumption in individual areas of the household such as information technology, lighting, etc. based on (EnergieAgentur.NRW 2011) (see Fig. 3.1).

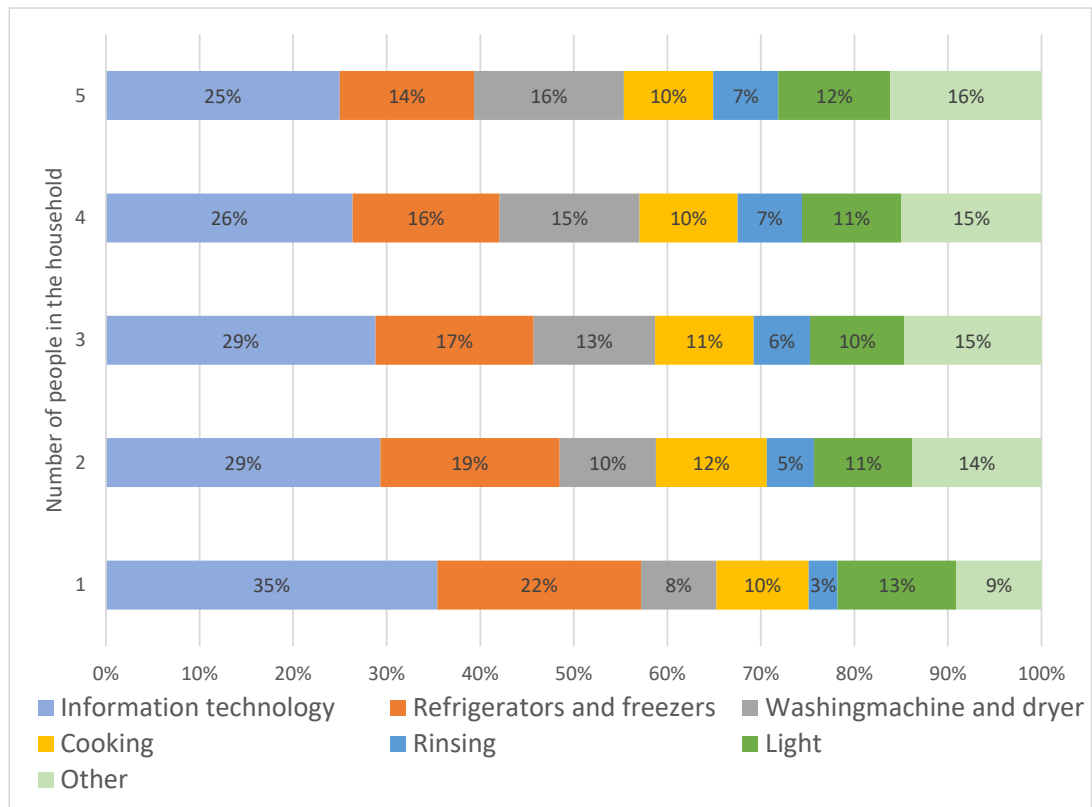


Fig. 3.1: Use of electricity in individual areas of households depending on number of people in household

Own figure based on EnergieAgentur.NRW (2011)

Even though each individual load profile is unique with traceable peaks, the sum of a large number of generated load profiles still corresponds to the typical standard load profile according to (BDEW 2017). The BDEW load profiles are differentiated by season (summer,

transition period, winter) and day of the week (weekday, Saturday, Sunday). Fig. 3.2 shows nine standard load profiles per day.

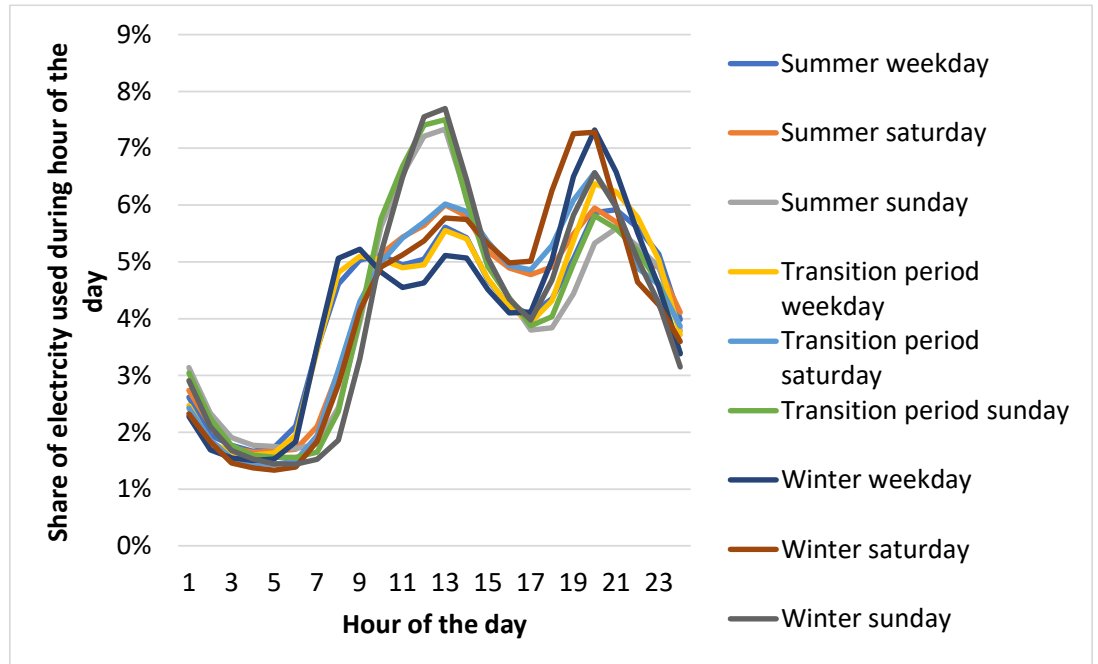


Fig. 3.2: Standard load profile

Own figure based on (BDEW 2017)

The user can select the number of people living in the household and the efficiency class of the household based on Stromspiegel (2017). The sum of the bottom-up load profiles corresponds to the demand of the selected efficiency class and household size (see Fig. 3.3)

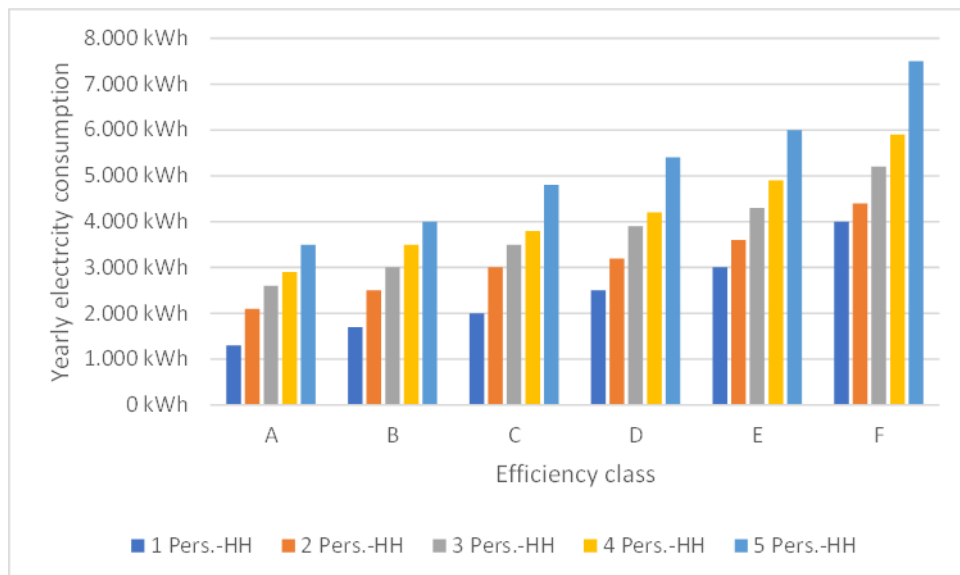


Fig. 3.3: Yearly consumption

Own figure based on Stromspiegel (2017)

4 Simulation of heat production and storage

This chapter gives an overview of the modules for heating. In general heating and electricity are separate parts of the model. But there are some interdependencies. On the one hand some of the heating technologies, esp. heat pumps, consume electricity and this will be part of the electricity consumption in the model. On the other hand the usage of some heating technologies can be dependent on the production of renewable energies. These details are explained in this chapter among the implementation and data basis of the technologies in general.

4.1 Control

The EProM thermal model consists of four components (see Fig. 4.1):

- **Heat production units:** Includes models for different heat production technologies, e.g., solar thermal, heat pump, condensing boiler.
- **Thermal storage:** Thermal storage with different layers.
- **Heat consumer:** There is a heating demand for both space heating and hot water heating.
- **Flow temperature:** Heater flow and heater return flow.

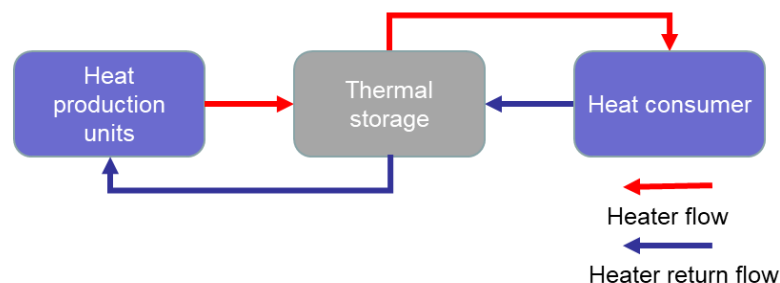


Fig. 4.1: Modeled heating components in EProM

Central elements for the control of heat production units are the thermal storage (see Chapter 4.3) and the flow temperatures. Based on the heating demand of the heat consumers (see Chapter 3.1), the required flow temperature is calculated (see calculation in the heating circuit in Chapter 4.2.2). If the heat stored in the thermal storage is not sufficient to meet the heating demand, additional heat production units start producing heat. While a solar thermal unit is always running, other technologies such as a heat pump, condensing boiler and electric heater can be switched on and off. However, the user can set certain constraints for the heat production units, such as minimum operation time or downtime.

When different heating technologies are present, there is a sequence in which the heating technologies are turned on. As described, a solar thermal collector is always producing heat when solar radiation is present. In a constellation of a heat pump combined with a condensing boiler or a heat pump combined with an electric heating, the heat pump is turned on first.

Only if the heat pump does not produce enough heat to meet the demand, a condensing boiler or electric heater is switched on. In combination with a photovoltaic production unit, the user can specify that heating production units are turned on to store extra heat in the thermal storage when electricity would otherwise be fed into the grid.

The following chapters describe the different components of the heating model in more detail.

4.2 Heating circuit

The space heating demand is met by the heating circuit. Fig. 4.2 shows a simplified flowchart of the heating circuit. Based on the heating demand, air temperature, user specifications and the temperature of the storage, the supplied heat and the heat deficit are calculated. A detailed description of the inputs and calculations follows.

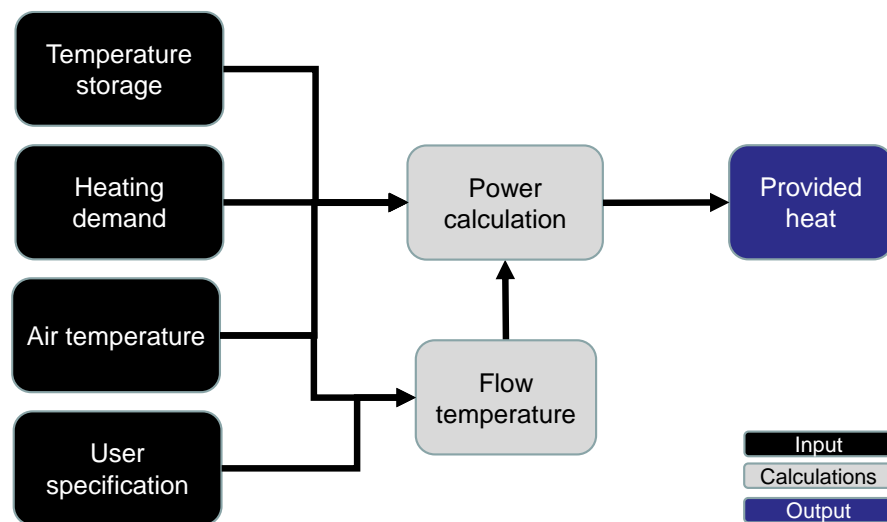


Fig. 4.2: Heating circuit flowchart

4.2.1 Input

The simulation of the heating circuit uses various inputs:

- **Heating demand:** See Chapter 3.1.
- **Air temperature:** Air temperature at location of the heating circuit (see Chapter 2.1).
- **User specification:** The user can make various specifications regarding the heating circuit:
 - Oversizing factor: Heating surfaces are often oversized because there has been an improvement in the building compared to the time when the heating surfaces were built, such as better insulation or better windows. This is taken into

account. As a default an oversizing factor of 1.2 based on Diefenbach et al. (2002) is taken into account.

- Various factors related to standard indoor temperature, type of radiator exponent (e.g. radiators, floor heating), maximum and minimum supply/return flow temperatures. The default values are taken from DIN V 4701-10:2003 (DIN e.V. 2003).
- Standard outdoor temperature: Standard outdoor temperature from Berlin-Lindenbergr is used by default (see Bundesverband Wärmepumpe e.V. 2023).
- **Temperature storage:** Top layer storage temperature.

4.2.2 Flow temperature

Based on DIN V 4701-10:2003, a flow temperature required to satisfy the heating demand is calculated for each time step. In contrast to DIN V 4701-10 calculations, time-varying values are calculated instead of mean values. In addition, an oversizing factor of 1.2 is added to the calculations according to the calculations of Diefenbach (2002). Eq. 4.1 shows the calculation.

Eq. 4.1: Flow temperature in the heating circuit according to DIN V 4701-10

$$\vartheta_{HF} = \vartheta_{HL}^{\frac{1}{n}} * (\vartheta_{HF,max} - \vartheta_{HF,min}) + \vartheta_{HF,min}$$

$$\vartheta_{HR} = \vartheta_{HL}^{\frac{1}{n}} * (\vartheta_{HR,max} - \vartheta_{HR,min}) + \vartheta_{HR,min}$$

$$\vartheta_{HP} = \frac{1}{f_{o,HC}} * \frac{\vartheta_{i,norm} - \vartheta_o}{\vartheta_{i,norm} - \vartheta_{u,min}}$$

ϑ_{HF} temperature heating flow

ϑ_{HL} heating circuit load

n type of heating: radiator: 1.3; floor heating:1.1

$\vartheta_{HF,max} / \vartheta_{HF,min}$ max/min heating flow temperature

ϑ_{HR} temperature heating return flow

$\vartheta_{HR,max} / \vartheta_{HR,min}$ max/min heating return flow temperature

ϑ_{HP} average heating circuit load

$f_{o,HC}$ oversizing factor heating circuit

$\vartheta_{i,norm}$ norm temperature inside

$\vartheta_{u,min}$ min temperature during heating period

ϑ_o norm temperature during heating period

4.2.3 Power calculation

Only when the air temperature is lower than the flow temperature (see Chapter 4.2.2) and the storage temperature is higher than the calculated return flow temperature, the heating circuit delivers heat. If both conditions are met, the heating demand is scaled to W/min based on the annual heating demand and the load profile (see Chapter 3.1).

Based on the temperature difference and the storage temperature, the heat supplied or not supplied is calculated. If the temperature of the storage is higher than the required flow temperature, the entire heating demand can be supplied by the heating circuit. If the storage temperature is lower than the flow temperature of the heating circuit, only part of the heating demand can be supplied. The heat supplied is calculated according to Eq. 4.2.

Eq. 4.2: Power calculation in the heating circuit

$$\dot{Q} = \frac{\vartheta_S - \vartheta_{HR}}{\vartheta_{HF} - \vartheta_{HR}} * \dot{q}$$

\dot{Q} provided heat

ϑ_S temperature storage

ϑ_{HR} temperature heating return flow

ϑ_{HF} temperature heating flow

\dot{q} heating demand

4.3 Thermal storage

The modeled thermal storage is based on Eicker (2012). Different layers within the thermal storage are modeled. Incoming and outgoing heat flows of the thermal storage are assigned to the different layers of the thermal storage. The temperature inside the layers is calculated taking into account the user specification, heat losses to the environment and convection between the layers. Fig. 4.3 shows a simplified flowchart of the thermal storage.

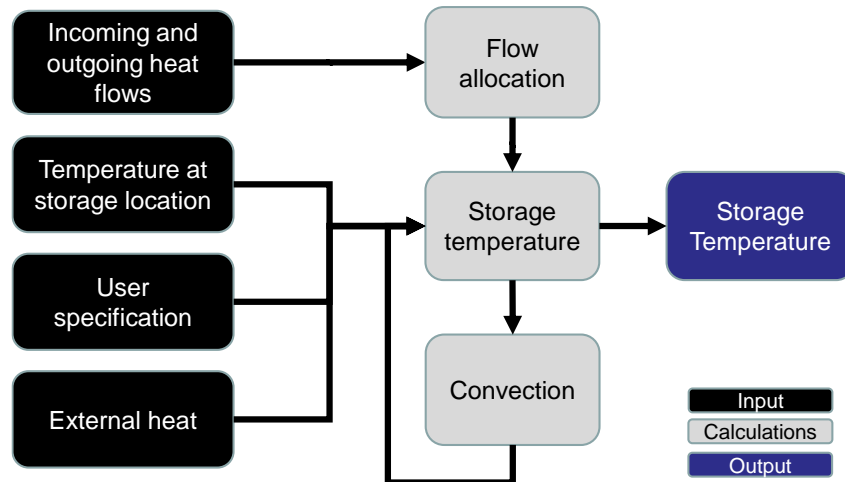


Fig. 4.3: Thermal storage flowchart

4.3.1 Input

The simulation of the thermal storage uses several inputs:

- **Incoming and outgoing heat:** Thermodynamic vectors containing flow temperature, mass flow, and heat capacity of water come from the various heat production technologies and the heating circuit.
- **Temperature at storage location:** The temperature at the location of the storage is kept constant throughout the year, assuming that the storage location is in a place, such as a basement, where the ambient temperature is nearly constant throughout the year. The default is 15°C.
- **User specification:** Radius and height of storage, maximum heat of storage, number of layers, starting temperature of storage, heat transfer coefficient of thermal storage and heat conductivity inside the thermal storage.
- **External heat:** Heat provided by electric heating (see Chapter 4.4.).

4.3.2 Flow allocation

Incoming and outgoing flows are being assigned to the appropriate layer where the temperature of the layer is closest to the flow temperature. It is assumed that the temperature in each layer is homogeneous. Therefore, incoming and outgoing flows can be assigned to exactly one layer.

4.3.3 Convection

A distinction is made between natural convection and forced convection. Natural convection occurs by heat convection from warmer to colder layers, and forced convection occurs when water is forced from one layer to another when incoming heat flows exceed outgoing flows in a layer (see Chapter 4.3.2). Eq. 4.3 is used to calculate natural convection.

Eq. 4.3: Natural convection from one layer to another according to Eicker (2012)

$$\dot{Q}_{f,i} = A_q * \frac{\lambda_{eff}}{Z} * (T_{i+1} - 2T_i + T_{i-1})$$

$\dot{Q}_{f,i}$ natural convection in layer i

A_q area of cross-section

λ_{eff} heat conductivity inside of the thermal storage

T_{i+1} temperature of layer $i + 1$

T_{i-1} temperature of layer $i - 1$

$2 T_i$ temperature of layer i

Three assumptions about the layers cause or influence a forced convection between the layers:

1. the heat capacity in each layer is constant (constant volume or mass),
2. the heat capacity of the water is constant and does not depend on the temperature of the water
3. there is heat conduction between the layers.

Starting with the warmest layer, the balance of incoming and outgoing heat flows determines whether water flows out to a colder layer or from a colder layer to a warmer layer. Mixed water flows from warmer and colder layers are transferred as a mixture to the corresponding layer, i.e., mass flows are added and the mixing temperature is calculated. (see Eq. 4.4)

Eq. 4.4: Forced convection from one layer to another according to Eicker (2012)

$$\dot{Q}_{e,i} = \dot{m} c_i * (T_{i-1} - T_{i+1})$$

$\dot{Q}_{e,i}$ natural convection in layer i

\dot{m} mass

c_i heat capacity of water in layer i

T_{i-1} temperature of layer $i - 1$

T_{i+1} temperature of layer $i + 1$

4.3.4 Storage temperature

The storage temperature in each layer is calculated based on Eicker (2012) and takes into account convection (see Chapter 4.3.3), heat losses to the environment, external heat from an electric heater, and incoming and outgoing flows (see Eq. 4.5).

Eq. 4.5: Storage temperature development over time for each layer according to Eicker (2012)

$$mc * \frac{dT_i}{dt} = \dot{Q}_{k,i} + \dot{Q}_{h,i} - \dot{Q}_{l,i} - \dot{Q}_{v,i} + \dot{Q}_{f,i} - \dot{Q}_{e,i}$$

dT_i temperature of layer i

M mass

c heat capacity of water

$\dot{Q}_{k,i}$ heat flow incoming in layer i

$\dot{Q}_{h,i}$ heat provided by external heat (e.g., electric heater) in layer i

$\dot{Q}_{l,i}$ heat flow outgoing in layer i

$\dot{Q}_{v,i}$ heat losses to environment in layer i

$\dot{Q}_{f,i}$ natural convection in layer i

$\dot{Q}_{e,i}$ forced convection in layer i

Losses to the environment are calculated using Eq. 4.6.

Eq. 4.6: Losses to the environment according to Eicker (2012)

$$\dot{Q}_{v,i} = U_{eff} * A_i * (T_i - T_0)$$

$\dot{Q}_{v,i}$ heat losses to environment in layer i

U_{eff} heat transfer coefficient of thermal storage

A_i enveloping surface

T_i temperature of layer i

T_0 temperature of storage location

Heat generated by an electric heater is evenly distributed to the different layers.

4.4 Electric heater

An electric heater is modeled to provide additional heat when other components cannot provide enough heat (see Chapter 4.4). It is assumed that the electric power is converted into thermal heat without any losses and the electric rod heats all layers of the thermal storage evenly. Therefore, in addition to the capacity of the electric heater, the user's specification as an input mainly influences the control:

- storage temperature at which the electric heater is switched on or off,
- the possibility to operate the electric heater at partial load and
- the impulse to turn on the electric heater when there is excess solar power that would otherwise be fed into the grid.

4.5 Condensing boiler

Fig. 4.4 shows a simplified flowchart of the simulation of the heat production of the condensing boiler. Heat production from the condensing boiler uses air temperature, heating demand, manufacturer information, and user specifications, and calculates the heat produced, the fuel energy consumed and the electricity required based on the utilization rate and power calculation. A detailed description of the inputs and calculations follows.

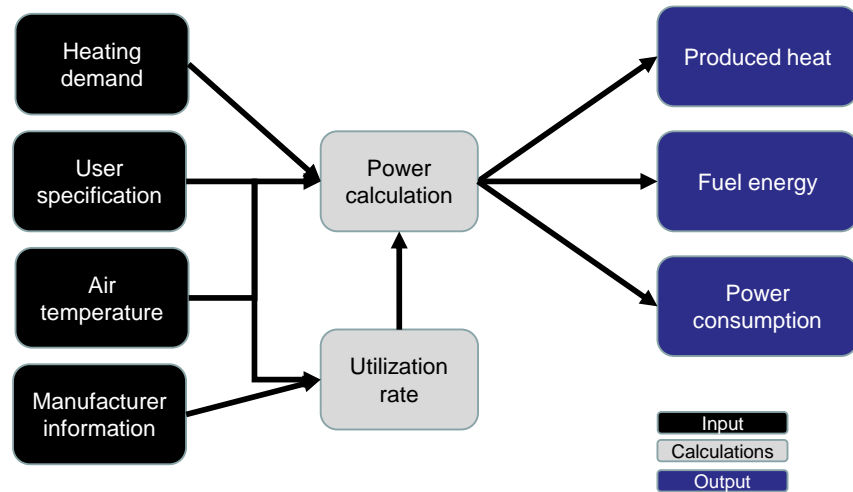


Fig. 4.4: Condensing boiler flowchart

4.5.1 Input

The simulation of the heat production of the condensing boiler uses different inputs:

- **Heating demand:** Indicates whether the condensing boiler should produce heat.
- **User specification:** Thermal and electrical power of the condensing boiler, minimum operating time.
- **Manufacturer information:** The default condensing boiler is the Vitocrossal 300 from Viessmann (2023a). Utilization rates for different air temperatures and firing rates are based on Viessmann (2006).
- **Air temperature:** Air temperature at the location of the condensing boiler (see Chapter 2.1).

4.5.2 Utilization rate

The utilization rate of the condensing boiler depends on the air temperature and the flow temperature in the heating circuit. The flow temperature is specified by the user. The air temperature depends on the location of the condensing boiler (see Chapter 2.1). The maximum utilization rate is used according to Vitocrossal 300 (Viessmann 2023a). The utilization rate at different air and flow temperatures is calculated according to Viessmann (2006) and Viessmann (2023a) (see Fig. 4.5).

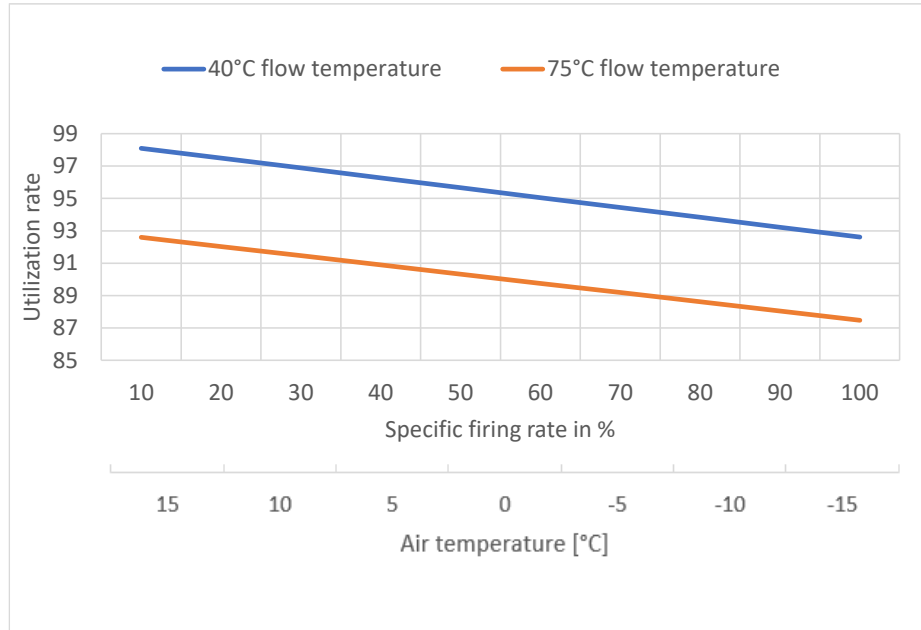


Fig. 4.5: Utilization rate of condensing boiler

Own calculations according to Viessmann (2006) and Viessmann (2023a). The firing rate increases with decreasing temperature.

4.5.3 Power calculation

When there is a signal for heating demand (see Chapter 0), the heat produced, the fuel energy required and the power consumption are calculated. The produced heat depends on the user's specification of the thermal power and the specific firing rate. The specific firing rate is based on Viessmann (2006) and Viessmann (2023a). The electrical consumption is determined by the user's specification of the electrical power of the condensing boiler and is by default according to Vitocrossal 300 (Viessmann 2023a). The fuel energy consumed is determined by the utilization rate divided by the utilization rate calculated (4.5.2). In addition, the low-temperature heating cannot be switched on for an arbitrary short period of time, the minimum operation time is determined by the minimum operation time of the condensing boiler. The heat produced, the energy used and the power consumption are calculated and the heat going to the storage is stored in a thermodynamic vector.

4.6 Heat pump

Fig. 4.6 shows a simplified flowchart of the heat pump's heat production. The heat production of the heat pump is calculated on a minute-by-minute basis using various inputs related to air, ground, and water temperatures, manufacturer information, and user specifications of the heat pump. The output of this module is the electricity demand and a thermodynamic vector containing flow temperature, mass flow, and heat capacity of water. A detailed description of the inputs and calculations follows.

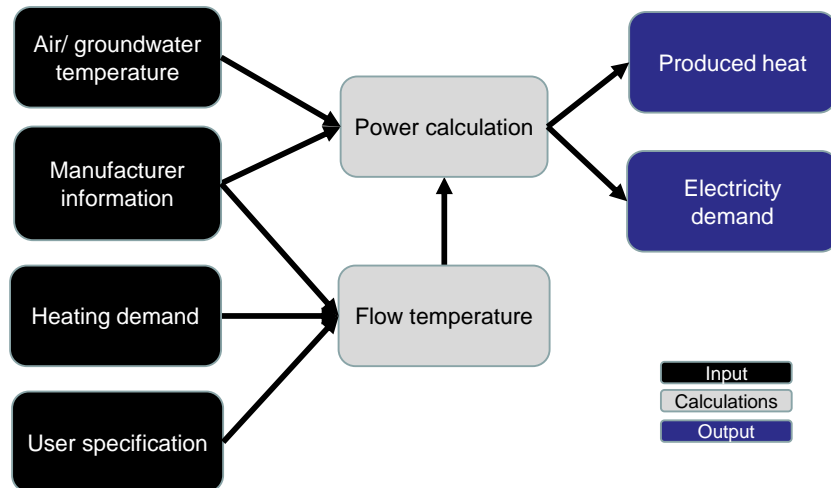


Fig. 4.6: Heat pump flowchart

4.6.1 Input

- **Manufacturer information:** Manufacturer information on coefficient of performance (COP), minimum and maximum temperature that the heat pump can provide. For the air-to-water heat pump, there is manufacturer information for three different heat pump implementations (Dimplex 6 KW (Dimplex 2023a), Dimplex 9 KW (Dimplex 2023b) and Nibe 8KW (NIBE 2023)) that the user can choose from. The default heat pump is the Dimplex 6 KW. For the water-to-water heat pump a Novelan-WIC10HXE (Novelan 2023a) is implemented and for a brine-to-water heat pump the Novelan SIC12.2H (Novelan 2023b) heat pump is used.
- **User specification:** Dimensioning, required temperature difference between flow temperature of heat pump and heating circuit, type (air-water, water-water, brine-water).
- **Air/groundwater temperature:** see Chapter 2.1.
- **Heating demand:** Indicates whether the heat pump is required for heat production and what the required flow temperature of the heat pump is.

4.6.2 Flow temperature

Before simulating the heat pump, the required flow temperature is determined. This is limited by the maximum and minimum flow temperature of the heat pump. In addition, the flow temperature must correspond to the required temperature difference. The required flow temperature results from the heating demand (see Chapter 3.1).

4.6.3 Power calculation

Based on the flow temperature and manufacturer's specifications, the required electricity and the produced heat are interpolated using the heat pump manufacturer's specifications.

4.7 Solar thermal

Fig. 4.7 shows a simplified flowchart of the solar thermal heat production. Solar thermal heat production is calculated on a minute-by-minute basis using various inputs related to global radiation on the collector, air temperature, manufacturer information, user specifications, and storage temperature. The output of this module is the electricity demand and a thermodynamic vector containing flow temperature, mass flow and heat capacity of the water. A detailed description of the inputs and calculations follows.

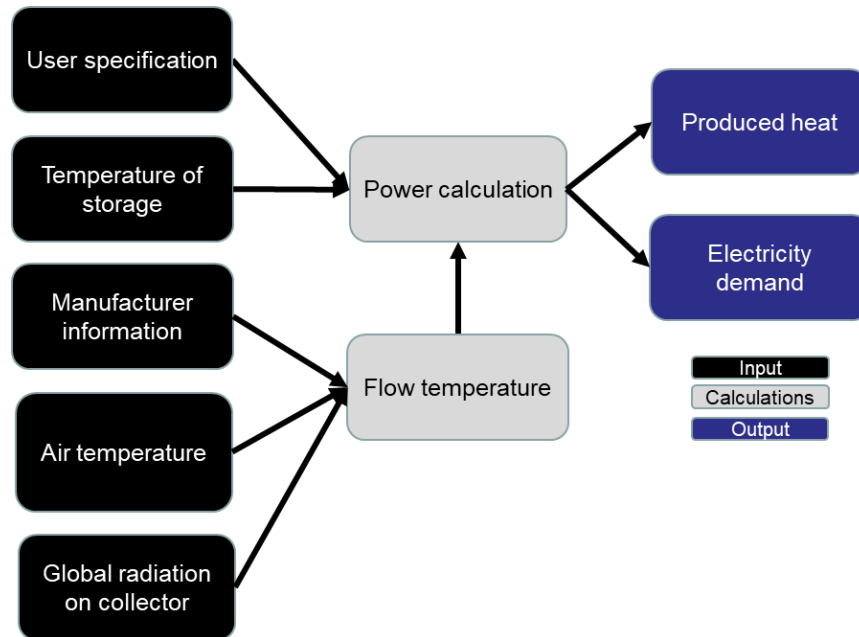


Fig. 4.7: Solar thermal flowchart

4.7.1 Input

The simulation of heat with the solar thermal collector uses several inputs:

- **Global radiation and air temperature:** Radiation and air temperature at the location of the solar thermal collector (see Chapter 2.1).
- **User specification:** Azimuth, incidence and area of the collector.
- **Storage temperature:** Temperature of the flow leaving the thermal storage (see Chapter 4.3).
- **Manufacturer information:** The Vitosol 100 from Viessmann is implemented as default (Viessmann 2023b; Müller-Steinhagen 2003).

4.7.2 Flow temperature

Parameters from manufacturer's information, global radiation, air temperature and user specification are included in the calculation of flow temperature using Eq. 4.7 (see Müller-

Steinhagen 2003). The empirical parameters $c_1, c_2, c_5, F'(\tau\alpha)_{en}, b_0, K_{\theta b}(\theta)$ und $K_{\theta d}(\theta)$ for the Vitosol 100 thermal collector are used from Müller-Steinhagen (2003).

Eq. 4.7: Dynamic collector model based on Müller-Steinhagen (2003)

$$\dot{q} = F'(\tau\alpha)_{en} * (K_{\theta b}(\theta) * G_b + K_{\theta d} * G_d) - c_1 * (\vartheta_m - \vartheta_a) - c_2 * (\vartheta_m - \vartheta_a)^2 - c_5 * \frac{d\vartheta_m}{dt}$$

$F'(\tau\alpha)_{en}$	conversion factor of direct irradiance
G_b, G_d	direct, diffuse irradiance
$K_{\theta b}, K_{\theta d}$	incident-angle-correction-factor of direct diffuse irradiance
c_1	thermal transmittance
c_2	temperature-dependent heat capacity of the collector
c_5	area-related heat capacity of the collector
ϑ_m	average fluid temperature inside of collector
ϑ_a	ambient temperature
θ	angle of incidence of direct irradiance
b_0	factor for determining the incidence-angle-correction-factor

4.7.3 Power calculation

To calculate the heat produced, the temperature difference between the state before ϑ_2 and after ϑ_1 heating in the solar thermal system was first calculated. ϑ_2 is equal to the storage temperature. With this temperature difference and the specific heat capacity c , the specific enthalpy can be calculated. From this, the heat energy produced can be calculated using the mass flow as a function of the collector area. This formula, Eq. 4.8, is shown below. It is derived from Quaschnig (2013).

Eq. 4.8: Produced heat of solar thermal according to Quaschnig (2013)

$$\dot{Q} = (\vartheta_2 - \vartheta_1) * c * \dot{m} * A$$

\dot{m} mass flow $\frac{kg}{s m^2}$

ϑ_2 temp. before heating in the solar thermal system K

ϑ_1 temp. after heating in the solar thermal system K

c specific heat capacity $4.2 \frac{kJ}{kg K}$

A collector area m^2

5 Simulation of electricity production and storage

5.1 Photovoltaic

Fig. 5.1 shows a simplified flowchart of the simulation of the electricity production with a photovoltaic (PV) module. Using various inputs regarding radiation, air temperature, manufacturer information, and user specification of the PV module and the inverter, the electricity production of the PV module is calculated on a minute-by-minute basis. The output of this module is the power production. A detailed description of the inputs and calculations follows.

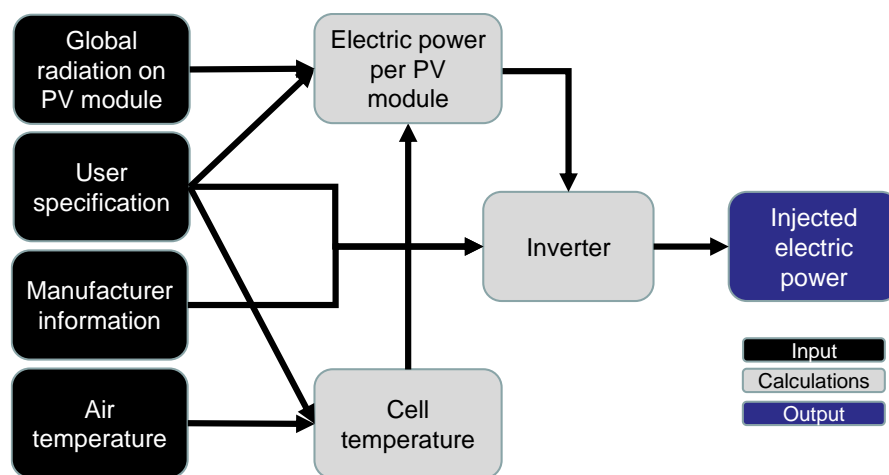


Fig. 5.1: Photovoltaic electricity production flowchart

5.1.1 Input

The simulation of electricity production with the photovoltaic panel uses different inputs:

- **User specification:** Azimuth, inclination, PV module size (in kWp), installation type (ventilation of PV-module) and inverter size.
- **Global radiation and air temperature:** Radiation and air temperature at the location of the PV panel (see Chapter 2.1).
- **Manufacturer information:** The default PV panel used is the PV panel S-Energy SM-255PC8 (S-Energy 2023). Furthermore, the solar panels MonoHyundai HiS-S310RG (Hyundai 2023) and Mono BL60UH 350W (ENF Solar 2023) can be selected. The default inverter is SMC8000TL (SMA Solar Technology AG 2023).

5.1.2 Cell temperature

The cell temperature of the PV panel influences the amount of electricity produced (Quaschnig 2013). The cell temperature is described in a simplified way by a linear temperature model based on Quaschnig (2013), which includes the type of installation of the

collectors and the associated ventilation, the outside temperature and the global radiation. The constant of proportionality decreases with increasing ventilation. By default, the simulation assumes a roof installation with good rear ventilation ($c = 29$), but other types of ventilation can be selected. The cell temperature of the panel is calculated using Eq. 5.1.

Eq. 5.1: Cell temperature of the panel

$$\vartheta_C = \vartheta_A + c * \frac{G}{1000 \frac{W}{m^2}}$$

ϑ_A ambient temperature

c constant of proportionality of specific solar module

G global radiation

5.1.3 Electric power

The performance of the photovoltaic system and the inverter is simulated according to the model of Sauer (1994) and approaches of Quaschnig (2013). Several parameters are used to simulate the performance of the PV module. These include global radiation, cell temperature and empirical data from manufacturer's fact sheets. Empirical data includes the temperature coefficient of the maximum power point voltage and support points determined from I-V curves of manufacturer's fact sheets. For the support points, the maximum current and voltage at a reference temperature of 25° Celsius for 0 W, 200 W, 600 W and 1000 W are determined from the manufacturer's fact sheets. Eq. 5.2

Eq. 5.2: Performance of the photovoltaic module at the maximum power point (Sauer 1994)

$$P_{MPP} = \frac{\alpha_1^2 * G^2}{\Gamma + \alpha_1 * G} * \left\{ \frac{\alpha_1 * \ln^2(G + 1) + \alpha_2 * \ln(G + 1) + \alpha_3}{\ln(G + 1) + \alpha_4} + c_T * (T_Z - T_{ref}) \right\}$$

G global radiation

α_i empiric parameter based on support points

c_T temperature coefficient of the maximum power point (MPP) voltage

T_Z cell temperature

T_Z cell reference temperature

Γ measure for the non-linearity of the current, empirically from support points

The calculated power is scaled up or down according to the determined size of the PV panel.

5.1.4 Inverter

The simulated PV panel produces direct current (DC). Therefore, an inverter must be simulated to convert the DC into alternating current (AC). Based on the data provided by the manufacturer of the inverter, the losses are calculated using the Schmidt-Modell (see Eq. 5.3) as described by Sauer (1994). The parameters v_{loss}^* , r_{loss}^* , p_{in}^* can be parameterized from three interpolation points. In this model the three support points applied are at 10 %, 50 % and 90 %.

Eq. 5.3: Inverter efficiency

$$\eta(p_{in}) = -\frac{1 + v_{loss}^*}{2 * r_{loss}^* * p_{in}} + \sqrt{\frac{(1 + v_{loss}^*)^2}{(2 * r_{loss}^* + p_{in})^2} + \frac{p_{in} - p_{self}^*}{r_{loss}^* * p_{in}^2}}$$

v_{loss}^* voltage losses proportional to the output power

p_{in}^* power independent no-load losses

r_{loss}^* ohmic losses that increase with the square of the current

The power injected into the grid is calculated by multiplying the calculated electric power by the efficiency of the inverter. The maximum injected power is limited by the size of the inverter.

5.2 Wind

Fig. 5.2 shows a simplified flowchart for simulating electricity production by a wind turbine. Using various inputs regarding wind speed, humidity, air pressure, and the specification of the wind turbine, the power produced from the wind turbine is calculated on a minute-to-minute basis. The output of this module is the power production in W per minute. A detailed description of the inputs and calculations follows.

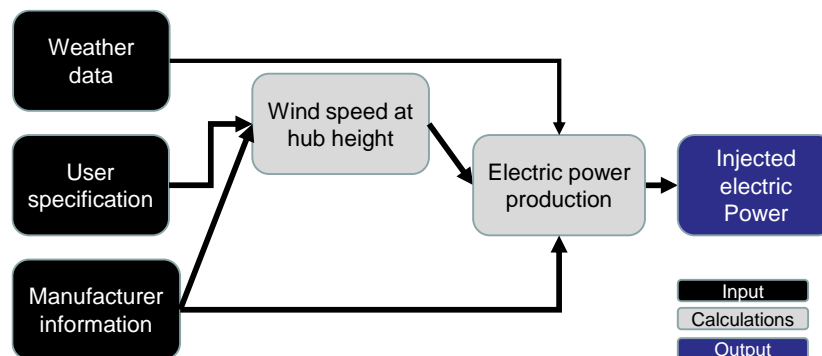


Fig. 5.2: Wind turbine flowchart

5.2.1 Input

The simulation of electricity production by the wind turbine uses several inputs:

- **Weather data:** Wind speed and air pressure.
- **User specification:** Hub height, rotor diameter, type of wind turbine (horizontal, small vertical wind turbine, large vertical wind turbine).
- **Manufacturer information:** Performance coefficients of the wind turbine at hub height: For small vertical wind turbines, a 100-W helical blade wind turbine with vertical axis is used as a default (Han et al. 2018), for small horizontal wind turbine, a Lely Aircon 30 is used (Lely Industries N.V. 2023), and for a large onshore wind turbine, a Vestas V136-4.2 MW (Vestas Wind System A/S 2023) is used.

Based on user's specifications regarding rotor diameter, rotor height and rotor type, the area of the rotor surface is calculated (see Eq. 5.4 and Eq. 5.5)

Eq. 5.4: Area of rotor surface of horizontal runner

$$A_R = d_R^2 * \frac{\pi}{4}$$

A_R rotor surface

d_R rotor diameter

h_R rotor height

Eq. 5.5: Area of rotor surface of vertical runner

$$A_R = 2 * h_R * d_R$$

5.2.2 Wind speed at hub height

Calculating the wind speed at hub height is necessary because the wind speed increases with height. The inputs of wind speed used in this simulation are made at a height of 10 m (see Chapter 2.1.). However, large wind turbines are more than 150 m high. To calculate the wind speed at hub height, Eq. 5.6 based on Hau (2016) is used. The equation takes into account the roughness of the environment where the wind turbine is located and the roughness of the area around the measurement. The roughness describes the influence of the surface condition or terrain structure on the wind speed. Tab. 5.1 shows an overview of the roughness factor according to the terrain. By default, the roughness of the measurement point z_1 is assumed to be 0.2. The roughness at the location of the wind turbine z_0 is assumed to be 0.15.

Eq. 5.6: Wind speed at hub height (Hau 2016)

$$v_{h_2} = v_{h_1} * \frac{\ln * \frac{h_2}{z_{0_2}}}{\ln * \frac{h_1}{z_{0_1}}}$$

h_2 hub height

h_1 height at which average wind speed was measured

v_{h_1} average wind speed

z_{0_1}, z_{0_2} roughness at h_1 and h_2

Tab. 5.1: Roughness of different types of landscapes

Data based on Hau (2016)

Z0 (m)	Type of the terrain
1	City, forest
0.5	Suburb
0.3	Built up area
0.2	Many trees and/or bushes
0.1	Agricultural land with closed appearance area
0.05	Agricultural land with open appearance area
0.03	Agricultural land with land with few buildings, trees etc.
0.01	Airport-runway, pasture grass
5*10 ⁻³	Bare soil (smooth)
10 ⁻³	Snow surface (smooth)
3*10 ⁻⁴	Sand surface (smooth)
10 ⁻⁴	Water areas (sea, lakes, fjords)

5.2.3 Electric power

If the wind speed (see Chapter 5.2.2) is greater than the minimum wind speed required according to manufacturer, then the electric power production is calculated using Eq. 5.7: .

Eq. 5.7: Produced electric power according to Hau (2016)

$$P_{el} = \frac{1}{2} * \rho_L * A_R * v_{h2}^3 * c_p$$

P_{el} electrical power

ρ_L air density

A_R area of rotor

v_{h2} wind speed at hub height

c_p coefficient of performance at hub height

The coefficient of performance at hub height is derived from the manufacturer's data sheets.

5.3 Battery

A simplified model is used for the simulation of batteries. User's specifications for capacity, maximum charge power, and battery efficiency, as well as simulated electricity flows in the use case, determine whether the battery is charged or discharged. Lifetime degradation is not included.

5.3.1 Input

The simulation of charging and discharging uses different inputs:

- **User specification:** Capacity, maximum charge power, battery efficiency.
- **Power demand and production:** Power demand and production at each time step of the simulation according to calculations in other modules.

5.3.2 Charging and discharging of the battery

The battery storage system is simplified. At each time step, electricity production and electricity demand of the use case are compared. If the electricity production is higher than the electricity demand and the battery is not fully charged, the battery is charged. If the electricity demand is greater than the electricity production and the battery is at least partially charged, the battery is discharged.

The charge and discharge power is limited to an upper level by a minimum function and a maximum function for discharging, taking into account the maximum charging power specified by the user. Self-discharge during the day and conversion losses are both reflected in the selected battery efficiency.

6 Output and post-processing

The main output of the model are time series objects with a fixed time step size of 60 seconds. As described in detail in the previous chapters, each modeled module has an individual output. Either this output is needed for further calculations in other modules (e.g. storage temperatures in the thermal storage are used as a control input in heat production units like the condensing boiler), the output is the desired result (e.g. the condensing boiler indicates how much fuel is needed as an input), or the output is used in post processing calculations.

In previous applications, the main use of EProM was the calculation of self-consumption shares and exchange with the grid, which is used for economic and ecological calculations. The time series of the generation added to the time series of the consumption gives the grid demand (excess of demand over generation) and the electricity fed into the grid (excess of generation over demand) at each time step. The difference between produced electricity and injected electricity quantifies the self-consumed electricity.

In a post-processing ecological evaluation, the electricity drawn from the grid can be evaluated with CO₂ emission per kWh in accordance with the shares of the electricity production units in the grid (e.g. Capros et al. 2016) and the respective footprints of these production units (e.g. Schlömer et al. 2014). The self-consumed electricity has to be evaluated accordingly with the respective footprints of the implemented energy production units. Thus, the simulation can be used to calculate the footprint of a household or neighborhood with different shares of implemented production and storage applications. Examples of these calculations can be found in Ouanes et al. (2022) and in Doračić et al. (2020).

In post-processing economic evaluations, use cases with different economic and regulatory frameworks can be calculated. Thus, different use cases can be calculated using costs of production units, electricity prices for electricity drawn from the grid and revenues for electricity fed into the grid. Examples of such calculations can be found in Doračić et al. (2020) and in Wiesenthal et al. (2022).

7 References

- Augustine, John (2017): Basic measurements of radiation at station Fort Peck (2017-08). *NOAA - Air Resources Laboratory, Boulder*. PANGAEA. <https://doi.pangaea.de/10.1594/PANGAEA.880923>.
- BDEW (2017): Standardlastprofile Strom. 1. January. Website: <https://www.bdew.de/energie/standardlastprofile-strom/> (accessed: 18. July 2023).
- BDEW (2022): BDEW/VKU/GEODE Leitfadens Abwicklung von Standardlastprofilen Gas. 31. March. Bundesverband Wärmepumpe e.V. (2023): Klimakarte. Website: <https://www.waermepumpe.de/normen-technik/klimakarte/> (accessed: 6. January 2023).
- Capros, P., A. De Vita, N. Tasios, P. Siskos, M. Kannavou, A. Petropoulos, S. Evangelopoulou, M. Zampara, D. Papadopoulos, Ch Nakos, et al. (2016): EU Reference Scenario 2016 - Energy, transport and GHG emissions Trends to 2050. Other. Luxembourg: European Commission Directorate - General for Energy, Directorate - General for Climate Action and Directorate - General for Mobility and Transport, July. Website: https://ec.europa.eu/energy/sites/ener/files/documents/REF2016_report_FINAL-web.pdf (accessed: 18. July 2023).
- Dieckhoff, Christian (2017): *Energieszenarien: Konstruktion, Bewertung und Wirkung - "Anbieter" und "Nachfrager" im Dialog*.
- Diefenbach, Nikolaus, Tobias Loga, Rolf Born, Marc Großklos and Carsten Herbert (2002): Energetische Kenngrößen für Heizungsanlagen im Bestand. Institut Wohnen und Umwelt GmbH.
- Dimplex (2023a): System M. Manual. - Compact 4/6 kW. Website: <https://www.meinhausshop.de/media/pdf/meinhausshop-dimplex-041HOIAOW2-061HOIAOW4-mont-de.pdf> (accessed: 8. February 2023).
- Dimplex (2023b): System M Comfort C9/12 kW. Website: https://oxomi.com/catalog-media/10256119/e44afd83a1d73fdd47f814bf8c2556e0/catalog.pdf?name=System_M_Comfort_Cooling_09-12_kW_Warmwasser_Montage-und_Gebrauchsanweisung.pdf&inline=false (accessed: 8. February 2023).
- DIN e.V. (2003): DIN V 4701-10:2003.
- Doračić, Borna, Jan Knoefel and Nanda Naber (2020): Prosumers for the Energy Union: Report on local, national and EU scenarios.
- DWD Climate Data Center (CDC) (2019): Historische 10-minütige Stationsmessungen der mittleren Windgeschwindigkeit und Windrichtung in Deutschland Version 1. https://open-data.dwd.de/climate_environment/CDC/observations_germany/climate/10_minutes/wind/historical/BESCHREIBUNG_obsgermany_climate_10min_wind_historical_de.pdf;
- Eicker, Ursula (2012): *Solare Technologien für Gebäude: Grundlagen und Praxisbeispiele*. 2., vollständig überarbeitete Auflage. Studium. Wiesbaden: Vieweg + Teubner.
- EnergieAgentur.NRW (2011): Erhebung „Wo im Haushalt bleibt der Strom?“ Anteile, Verbrauchswerte und Kosten von 12 Verbrauchsbereichen in Ein- bis Sechs-Personen-Haushalten. https://1-stromvergleich.com/wp-content/uploads/erhebung_wo_bleibt_der_strom.pdf.
- ENF Solar (2023): BL60UH 335W-350W. Website: <https://cdn.enfsolar.com/Product/pdf/Crystalline/5d47c5364c889.pdf> (accessed: 6. January 2023).
- Eurostat (2017): File:Share of fuels in the final energy consumption in the residential sector for cooking. Website: [https://ec.europa.eu/eurostat/statistics-explained/index.php?title=File:Share_of_fuels_in_the_final_energy_consumption_in_the_residential_sector_for_cooking,_2017_\(%25\).png](https://ec.europa.eu/eurostat/statistics-explained/index.php?title=File:Share_of_fuels_in_the_final_energy_consumption_in_the_residential_sector_for_cooking,_2017_(%25).png) (accessed: 18. July 2023).
- Grubb, Michael, Jae Edmonds, Patrick ten Brink and Michael Morrison (1993): The Costs of Limiting Fossil-Fuel CO₂ Emissions: A Survey and Analysis. *Annual Review of Energy and the Environment* 18, Nr. 1 (November): 397–478.
- Haefelin, Martial (2017): Basic measurements of radiation at station Palaiseau (2017-02). *Laboratoire de Météorologie Dynamique du C.N.R.S., Ecole Polytechnique*. PANGAEA. <https://doi.pangaea.de/10.1594/PANGAEA.874312>.
- Han, Dowon, Young Heo, Nak Choi, Sang Nam, Kyoung Choi and Kyung Kim (2018): Design, Fabrication, and Performance Test of a 100-W Helical-Blade Vertical-Axis Wind Turbine at Low Tip-Speed Ratio. *Energies* 11, Nr. 6 (11. June): 1517.
- Hau, Erich (2016): *Windkraftanlagen*. Berlin, Heidelberg: Springer Berlin Heidelberg. <http://link.springer.com/10.1007/978-3-662-53154-9>.
- Hellwig, Mark (2003): Entwicklung und Anwendung parametrisierter Standard-Lastprofile. München: TU München, 15. September. <https://mediatum.ub.tum.de/doc/601557/601557.pdf>.

- Herbst, Andrea, Felipe Toro, Felix Reitze and Eberhard Jochem (2012): Introduction to Energy Systems Modelling. *Swiss Journal of Economics and Statistics* 148, Nr. 2 (April): 111–135.
- Hyundai (2023): Hyundai Solar Module. Website: <https://cdn.enfsolar.com/Product/pdf/Crystalline/5ce4cd280b79c.pdf> (accessed: 6. January 2023).
- IDAE (2011): SECH PROJECT -SPAHOUSEC Analyses of the energy consumption of the household sector in Spain FINAL REPORT. https://cros-legacy.ec.europa.eu/system/files/SECH_Spain.pdf (accessed: 18. July 2023).
- Instituto Nacional de Estadística (2008): Household and Environment Survey 2008 - Percentage of dwellings with a small household appliance, by level of studies completed by the reference person and type of small household appliance. *INE*. Website: <https://www.ine.es/jaxi/Datos.htm?path=/t25/p500/2008/p02/I0/&file=01217.px> (accessed: 18. July 2023).
- Jordan, Ulrike and Klaus Vajen (2003): DHWcalc Werkzeug zur Generierung von Trinkwasser-Zapfprofilen auf statistischer Basis.
- Knap, Wouter (2018): Basic and other measurements of radiation at station Cabauw (2018-06). *Koninklijk Nederlands Meteorologisch Instituut, De Bilt*. PANGAEA. <https://doi.pangaea.de/10.1594/PANGAEA.892185>.
- Lely Industries N.V. (2023): Lely Aircon LA30 Wind turbine. Website: https://www.lely.com/media/filer_public/06/cc/06ccbc10-b761-4b78-8e7d-b7d49a3ca1bd/summary_report_lely_aircon_30_de.pdf (accessed: 6. January 2023).
- Miara, Marek, Danny Günther, Thomas Kramer, Thore Oltersdorf and Jeannette Wapler (2012): Wärmepumpen Effizienz Messtechnische Untersuchung von Wärmepumpenanlagen zur Analyse und Bewertung der Effizienz im realen Betrieb. 30. September. Website: <https://docplayer.org/44798637-Waermepumpen-effizienz-messtechnische-untersuchung-von-waermepumpenanlagen-zur-analyse-und-bewertung-der-effizienz-im-realen-betrieb.html> (accessed: 25. July 2023).
- Müller-Steinhagen, H. (2003): Prüfbericht Wärmeleistung Sonnenkollektor. Forschungs- und Testzentrum für Solaranlagen Stuttgart. https://www.igte.uni-stuttgart.de/en/publications/publikationen-forschungs-und-testzentrum-fuer-solaranlagen-00001/dokumente_tzs/tests2003_inhalt.pdf.
- Nakata, Toshihiko (2004): Energy-economic models and the environment. *Progress in Energy and Combustion Science* 30, Nr. 4 (January): 417–475.
- NGWA (1999): Groundwater Temperature's Measurement and Significance. <https://www.ngwa.org/what-is-groundwater/About-groundwater/groundwater-temperature's-measurement-and-significance>.
- NIBE (2023): Luft-/Wasserwärmepumpe NIBE F2120. Website: <https://assetstore.nibe.se/hcms/v2.3/entity/document/22382/storage/MDIyMzgyLzAvbWFzZdGVy> (accessed: 8. February 2023).
- Novelan (2023a): Betriebsanleitung Wasser-Wasser Wärmepumpen. Website: https://www.novelan.at/fileadmin/content/downloads/06%20Wasser-Wasser/05%20Betriebsanleitung/83050703eDE_WIC.pdf (accessed: 8. February 2023).
- Novelan (2023b): Betriebsanleitung Sole-Wasser Wärmepumpen. Website: https://files.ait-group.net/FILES/Novelan/Betriebsanleitungen/01%20Waermepumpen/02%20Sole%20Wasser/04%20SIC/83056703gDE_SIC.pdf (accessed: 8. February 2023).
- Olano, Xabier (2017): Basic measurements of radiation at station Cener (2017-01). *National Renewable Energy Centre*. PANGAEA. <https://doi.pangaea.de/10.1594/PANGAEA.871654>.
- Ouanes, Nesrine, Jan Kegel, Jan Wiesenthal, Clara Lenk, Hannes Bluhm, Julika Weiß and Lukas Torliene (2022): Prosuming – energy sufficiency and rebound effects: Climate impact of changing household consumption patterns in Germany. *TATuP - Zeitschrift für Technikfolgenabschätzung in Theorie und Praxis* 31, Nr. 2 (18. July): 18–24.
- Perez, Richard, Pierre Ineichen, Robert Seals, Joseph Michalsky and Ronald Stewart (1990): Modeling daylight availability and irradiance components from direct and global irradiance. *Solar Energy* 44, Nr. 5: 271–289.
- Perez, Richard, Robert Seals, Pierre Ineichen, Ronald Stewart and David Menicucci (1987): A new simplified version of the perez diffuse irradiance model for tilted surfaces. *Solar Energy* 39, Nr. 3: 221–231.
- Perez, Richard and Ronald Stewart (1986): Solar irradiance conversion models. *Solar Cells* 18, Nr. 3–4 (September): 213–222.
- Quaschnig, V. (2013): *Regenerative Energiesysteme Technologie - Berechnung - Simulation*. 7. Auflage. München: Hanser Verlag.

- Reinhardt, Andreas, Paul Baumann, Daniel Burgstahler, Matthias Hollick, Hristo Chonov, Marc Werner and Ralf Steinmetz (2012): On the Accuracy of Appliance Identification Based on Distributed Load Metering Data. *Proceedings of the 2nd IFIP Conference on Sustainable Internet and ICT for Sustainability (SustainIT)*.
- Rovers, Ronald (2019): m2 living per capita in Europe, and consequences – Ronald Rovers. 24. February. <http://www.ronaldrovers.com/m2-living-per-capita-in-europe-and-consequences/> (accessed: 18. July 2023).
- Sauer, U. (1994): Untersuchungen zum Einsatz und Entwicklung von Simulationsmodellen für die Auslegung von Photovoltaik-Systemen. Technische Universität Darmstadt.
- Schlömer, S., T. Bruckner, L. Fulton, E. Hertwich, A. McKinnon, D. Percy, J. Roy, R. Schaeffer, R. Rims, P. Smith, et al. (2014): *Annex III: Technology-specific cost and performance parameters*. Climate Change 2014: Mitigation of Climate Change. Contribution of Working Group III to the Fifth Assessment Report of the Intergovernmental Panel on Climate Change. Cambridge, United Kingdom and New York, NY, USA: Cambridge University Press.
- S-Energy (2023): SM-255PC8. Website: <https://www.amerescosolar.com/wp-content/uploads/S-Energy-SM-250PC8.pdf> (accessed: 6. January 2023).
- SMA Solar Technology AG (2023): Sunny Mini Central 6000TL / 7000TL / 8000TL. Website: https://www.pvxchange.com/mediafiles/pvxchange/attachments/Datenblatt%20SMC6000TL_8000TL.pdf (accessed: 6. January 2023).
- Statistisches Bundesamt (2019): Wirtschaftsrechnungen Einkommens- und Verbrauchsstichprobe Wohnverhältnisse privater Haushalte. https://www.destatis.de/DE/Themen/Gesellschaft-Umwelt/Wohnen/Publikationen/Downloads-Wohnen/evs-wohnverhaeltnis-haushalte-2152591189004.pdf?__blob=publicationFile.
- Stromspiegel (2017): Stromspiegel 2017. https://www.stromspiegel.de/fileadmin/ssi/stromspiegel/Downloads/Stromspiegel_2017_web.pdf.
- van Thiel, Lisanne (2017): Rapport Watergebruik Thuis 2016. July. <https://www.vewin.nl/SiteCollectionDocuments/Publicaties/Cijfers/Watergebruik-Thuis-2016.pdf>.
- VDI (2017): *VDI 2067 Blatt 12 - Wirtschaftlichkeit gebäudetechnischer Anlagen - Nutzenergiebedarf für die Trinkwassererwärmung*. <https://www.vdi.de/richtlinien/details/vdi-2067-blatt-12-wirtschaftlichkeit-gebaeudetechnischer-anlagen-nutzenergiebedarf-fuer-die-trinkwassererwaer-mung>.
- Vestas Wind System A/S (2023): 4 MW Platform. Website: <https://nozebra.ipapercms.dk/Vestas/Communication/4mw-platform-brochure/?page=1> (accessed: 6. January 2023).
- Viessmann (2006): Brennwerttechnik. <https://docplayer.org/7593460-Fachreihe-brennwerttechnik-brennwerttechnik-fuer-wirtschaftlichkeit-und-umweltschonung.html>.
- Viessmann (2023a): Vitocrossal 300 - Datenblatt. Website: file:///ioew.local/userdirs/jan.wiesenthal/Downloads/DB-5796294_Vitocrossal_300_Typ_CM3C.pdf (accessed: 8. February 2023).
- Viessmann (2023b): Datenblatt Vitosol 100-FM. Website: <https://www.viessmann.de/de/produkte/solarthermie/vitosol-100-fm.html> (accessed: 8. February 2023).
- Wacker, Stefan and Klaus Behrens (2022): Basic measurements of radiation at station Lindenberg (1994-10 et seq). *Meteorologisches Observatorium Lindenberg - Richard-Aßmann-Observatorium*. PANGAEA. <https://doi.pangaea.de/10.1594/PANGAEA.946382>.
- Wiesenthal, Jan, Astrid Aretz, Nesrine Ouanes and Kristian Petrick (2022): *Energy Sharing: Eine Potenzialanalyse - Gemeinschaftlich Strom im Verteilnetz erzeugen und nutzen: Eine Studie zum Umsetzungsvorschlag im Rahmen von Artikel 22 der Erneuerbare-Energien-Richtlinie der EU*. https://www.ioew.de/fileadmin/user_upload/BILDER_und_Downloaddateien/Publikationen/2022/Energy_Sharing_Eine_Potenzialanalyse_1.pdf.
- Wiesenthal, Jan and Frieder Schnabel (2022): Multi-use of Community Energy Storage: Energy Services and their Compatibility with Increasing Self-consumption as Primary Service with a Focus on Germany. Event: International Renewable Energy Storage Conference 2021 (IRES 2021), Global Online Event, Germany. <https://www.atlantis-press.com/article/125970997>.
- Wilkinson, Mark D., Michel Dumontier, IJsbrand Jan Aalbersberg, Gabrielle Appleton, Myles Axton, Arie Baak, Niklas Blomberg, Jan-Willem Boiten, Luiz Bonino da Silva Santos, Philip E. Bourne, et al. (2016): The FAIR Guiding Principles for scientific data management and stewardship. *Scientific Data* 3, Nr. 1 (15. March): 160018.